Nanoscale

Volume 1 | Number 1 | Jan 2013 | Pages 1–100

Nanoscale

www.rsc.org/nanoscale

This is an *Accepted Manuscript*, which has been through the Royal Society of Chemistry peer review process and has been accepted for publication.

Accepted Manuscripts are published online shortly after acceptance, before technical editing, formatting and proof reading. Using this free service, authors can make their results available to the community, in citable form, before we publish the edited article. We will replace this *Accepted Manuscript* with the edited and formatted *Advance Article* as soon as it is available.

You can find more information about *Accepted Manuscripts* in the **Information for Authors**.

Please note that technical editing may introduce minor changes to the text and/or graphics, which may alter content. The journal's standard **Terms & Conditions** and the **Ethical guidelines** still apply. In no event shall the Royal Society of Chemistry be held responsible for any errors or omissions in this *Accepted Manuscript* or any consequences arising from the use of any information it contains.

ARTICLE TYPE

The unexpected effect of PEGylated gold nanoparticles on the primary function of erythrocytes

Zeng He,[a] **Jiaxin Liu***[a] **and Libo Du***[b]

Polyethylene glycol functionalized gold nanoparticles (PEGylated AuNPs) have been widely used as nano carrier for the delivery of various drugs. However, little attention has been paid on whether the PEGylated AuNPs could affect the primary function of human erythrocytes−the main cellular components in the blood. In the current study, we show that both the deformability and oxygen-delivering ability of erythrocytes are decreased when treated by PEGyalted AuNPs with different sizes, which can be attributed to the interaction
10 between PEGylated AuNPs and erythrocyte membrane. It is observed that the PEGylated AuNPs could also induce the aggregation of band-3 and the ATP decrease of erythrocytes. In addition, the PEGylated AuNPs can accelerate the loss process of CD47 on erythrocytes membrane, possibly enhancing the senescent process of erythrocytes and the following clearance by SIRPα-expressing leukocytes in bloodstream. The results suggested that PEGylated AuNPs have a potential to affect the primary function of human erythrocytes, which should be considered when using them as drug carriers.

Introduction

15 Polyethylene glycol functionalized gold nanoparticles (PEGylated AuNPs) are promising candidates in nanomedicine for a range of applications, from *in vivo* target imaging to drug delivery due to their unique properties including high
20 biocompatibility and long circulation time in blood [1-5]. As the extensive application of PEGylated AuNPs in the field of nanomedicine, the toxicity of PEGylated AuNPs has been attracted considerable attention in the past decade. It was reported that PEGylated AuNPs enhanced LPS-induced production of NO
25 and IL-6 and inducible nitric oxide synthase expression in RAW 264.7 cells, partially by activating p38 mitogen-activated protein kinases and nuclear factor-kappa B pathways[6]. Cho et al. showed that PEGylated AuNPs with small size not only can be entrapped in cytoplasmic vesicles and lysosomes of Kupffer cells,
30 macrophages of spleen, and mesenteric lymph node, but also could transiently activate CYP1A1 and 2B (phase I metabolic enzymes), which play a critical role in hepatic injury and protection, in liver tissues from 24 h to 7 days[7]. However, among these studies, most of which are only focused on the *in vitro*
35 cytotoxicity or *in vivo* pharmakinetic toxicity[8,9].

As known, the main components in the circulatory systems is erythrocytes, whose primary function is to carry oxygen from the lungs to the tissues throughout the body *via* the blood flow and transport carbon dioxide from tissues to the lungs, where it can be
40 breathed out[10]. For those drugs used in clinical, they are generally designed to administer through intravenous (i.v.) injection in order to increase their bioavailability. Apparently, these drugs would firstly interact with erythrocytes. Similarly, for nanodrugs based on PEGylated AuNPs, the erythrocytes are also one of the
45 first components that PEGylated AuNPs contact when they are entered into the body through i.v. injection. Therefore, beside the

in vitro cytotoxiciyt or *in vivo* pharmakinetic toxicity, it is necessary to evaluate whether the PEGylated AuNPs could affect the primary function of erythrocytes prior to their *in vivo*
50 application.

On the other hand, it has been demonstrated that the injected foreign substances can affect the primary function of erythrocytes and then would provoke redox imbalance, thereby leading to oxidative-stress related diseases[11]. As has been demonstrated
55 before, nanoparticles including hydroxyapatite, silica, TiO_2, magnetite, and polymers, as a foreign substance, could also play an adverse effect on erythrocytes through inducing oxidative damage, genotoxicity and cytotoxicity[12-15]. However, for PEGylated AuNPs, although a few studies revealed the effect of
60 PEGylated AuNPs on erythrocytes, which showed that PEG-coated AuNPs could bind and be uptaken by blood cells including platelets, erythrocytes, and white blood cells *in vivo*[16], the effect of PEGylated AuNPs on the primary function of erythrocytes remains unexplored. Based on the above description, it is of great
65 important to evaluate the influence of the PEGylated AuNPs on erythrocytes prior to their clinical application. Moreover, as different sizes of PEGylated AuNPs have different circulation time and targeting efficiency when used as drug carriers[17], it is also critical to evaluate the effect of different sizes of PEGylated
70 AuNPs on the function of erythrocytes. In this study, we employed three different sizes (4.5, 13 and 30 nm) of PEGylated AuNPs to investigate the effect of PEGylated AuNPs on the function of erythrocytes. Our studies may contribute to clarify the molecular mechanism underlying whether and how the
75 PEGylated AuNPs affect the function of erythrocytes and provide important biosafety information regarding the biomedical application of PEGylated AuNPs *in vivo*.

Results and discussion

***In vitro* hemolytic activity of PEGylated AuNPs.** For the intravenously administered pharmaceuticals, whether they can induce hemolysis must be firstly considered before further clinical application[18]. The term "hemolysis" is commonly used to
5 describe damage to erythrocytes leading to the leakage of the iron-containing protein hemoglobin into the bloodstream and cause potentially life-threatening conditions such as thrombosis and renal impairment[19]. Previous studies have demonstrated that the nature of the surface ligands on the AuNPs plays a critical
10 role in surface-functionalized AuNPs-induced hemolysis[19]. It is therefore necessary to evaluate whether PEGylated AuNPs is hemocompatible prior to *in vivo* application. To this end, we prepared three different sizes of PEGylated AuNPs (4.5 nm, 13 nm, 30 nm), as described in the supplementary information.
15 Transmission electron microscopy (TEM), which could provides the details about internal composition, images (Fig. 1b) and dynamic light scattering (DLS) (Fig. 1c) measurement showed that all the three nanoparticles were well monodispersed with average size of ~ 4.5 nm, 13 nm, and 30 nm, respectively. All
20 particles were then subjected to evaluate their hemolytic activities. As illustrated in Fig. 2a, all sizes of PEGylated AuNPs showed almost negligible hemolysis in comparison with negative control. Previous results also demonstrated that PEG functionalized AuNPs did not show any hemolysis activity
25 against human erythrocytes[20], which are coincident with our results. Thus, it can be inferred that the PEGylated AuNPs have good hemocompatiblility.
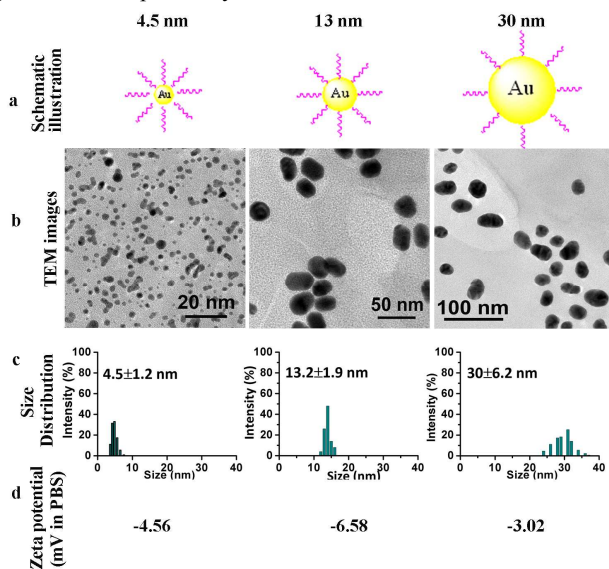
Figure 1. Characterization of PEGylated AuNPs with different
30 sizes. (a) Schematic illustration of the synthesized PEGylated AuNPs; (b) The transmission electron microscopy images of PEGylated AuNPs; (c) Size distribution of PEGylated AuNPs; (d) Zeta potential of PEGylated AuNPs in PBS.

35 **Effect of PEGylated AuNPs on erythrocytes deformability.** Although PEGylated AuNPs did not induce apparent hemolysis, the question remains whether PEGylated AuNPs could affect the other normal function of erythrocytes, i.e. deformability. The remarkable deformability property of erythrocytes, which

40 depends strongly on the flexibility of the cell membrane, is critical for effective blood flow and is considered as an essential
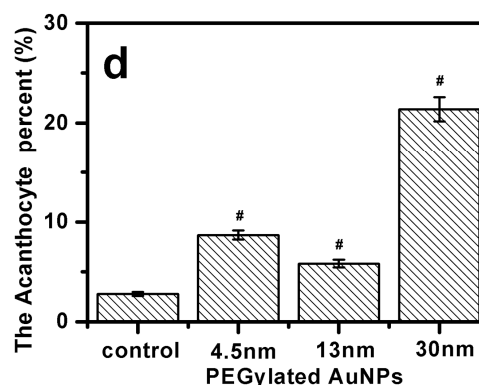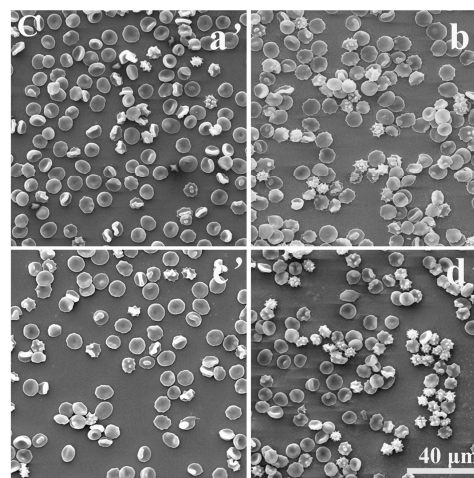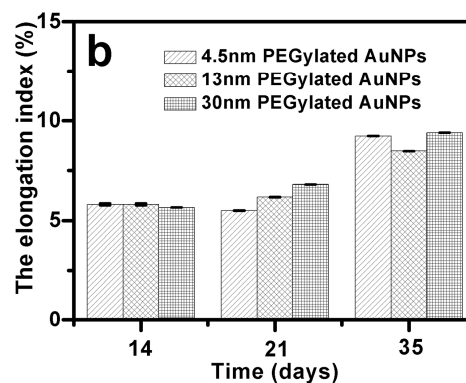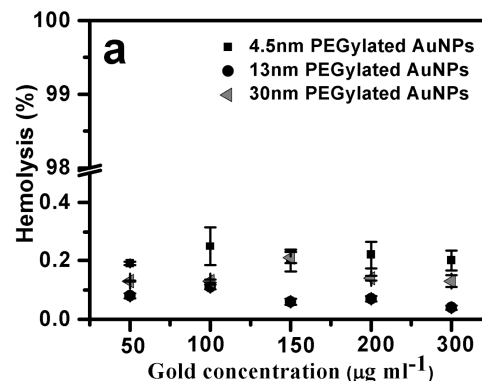
Figure 2. The hemolysis and deformability change of erythrocytes induced by PEGylated AuNPs. (a) Hemolysis rate of erythrocytes induced by different concentration of PEGylated AuNPs. Aliquots of erythrocyte suspension were pre-incubated
5 with PEGylated AuNPs for 4 h and then the hemolytic activity was determined (if not specified, the concentration refers to the concentration of gold elements); (b) The elongation index (at 1.54 Pa) of erythrocytes treated by the concentration of PEGylated AuNPs (200μg ml^{-1}) with different size. (c) The SEM images of
10 erythrocytes treated by different size PEGylated AuNPs. (a', control; b', erythrocytes treated by 4.5 nm PEGylated AuNPs; c', erythrocytes treated by 13 nm PEGylated AuNPs; erythrocytes treated by 30 nm PEGylated AuNPs; (d) The statistics of the SEM images. *$p<0.05$, #$p<0.01$

15

feature for their biological function. Surprisingly, although a few studies have investigated mesoporous silica particles or silver nanoparticle-induced haemolysis, membrane damage, etc[14,15], this potential problem has not been addressed for any PEGylated
20 AuNPs-based drug carrier, to the best of our knowledge. Thus, it is important to assess whether the deformability of erythrocytes is affected by PEGylated AuNPs. Moreover, as illustrated in the previous study[21], the i.v. injected PEGylated AuNPs could exist in the blood for about one month. Based on the above
25 consideration, to obtain the long term effect of PEGylated AuNPs on the erythrocytes, several different time intervals (1, 7, 14, 21, 35 days) were selected to evaluate the impact of PEGylated AuNPs on erythrocytes in our study. *Note: if there is no different between the control group and PEGylated AuNPs treated groups,*
30 *the results would not be shown in the current study.* As shown in Fig. 2b, for all sizes of PEGylated AuNPs, the deformability of erythrocytes (the elongation index of erythrocytes was used as the indicator for the deformability of erythrocytes) decreased with increasing incubation time at high shear stress of 1.54 Pa.
35 Considering previous studies demonstrated that the reduced deformability of erythrocyte may result in impaired perfusion and oxygen delivery in peripheral tissues[22,23], and rigid erythrocytes might directly block capillaries and disturb microcirculation[24], it can be reasonably inferred that the deformability of erythrocytes
40 induced by PEGylated AuNPs should be considered before their application *in vivo*.

Additionally, previous studies demonstrated that the nanoparticls (NPs)-regulated deformability of erythrocyte is usually associated with the interaction between NPs and
45 erythrocyte membrane[14,15]. We therefore speculated that the reason regarding the deformability of erythrocyte regulated by PEGylated AuNPs may also be attributed to the attachment of PEGylated AuNPs to the surface of erythrocytes, which subsequently restricts the flexibility of the membrane and leads to
50 impairment in the deformability of erythrocytes. Further considering that scanning electron microscopy (SEM) could provide details of the sample's surface and its composition, it can be reasonably speculated that the SEM may provide an ideal alternative approach for the study of erythrocytes deformability.
55 Therefore, to address the above hypothesis, the surface topography of erythrocytes treated by PEGylated AuNPs was measured by SEM. The SEM image (Fig. 2c) showed that at small size of PEGylated AuNPs, only a small percentage of

aberrant morphology can be observed, indicating that a small
60 proportion of PEGylated AuNPs was absorbed to the surface of erythrocytes. In contrast, a large proportion of PEGylated AuNPs with larger size attached to erythrocytes membrane and induced a strong local membrane deformation, which frequently resulted in particle encapsulation by erythrocytes. Moreover, the membrane
65 wrapping around PEGylated AuNPs may led to an echinocytic (spiculated) shape transformation of erythrocytes and a reduction in the ratio of surface area to volume[25]. In addition, previous studies illustrated that changes in the shape, mechanical characteristics or the integrity of erythrocytes have severe
70 implications for the functionality of the cell, as can be seen in several dysfunctional states of the erythrocytes, whether environmentally induced or due to hereditary defects or diseased states[26, 27]. As demonstrated in the Fig. 2, it can be concluded that the inability to maintain their normal surface area and the control
75 of their cell volume may ultimately lead to the destruction of these cells, even serious dieseases. To further verify these results, the Au contents in the PEGylated treated erythrocytes were detected by inductively coupled plasma mass spectrometry (ICP-MS). The Au concentrations in erythrocytes after pretreatment of
80 different sizes of PEGylated AuNPs were shown in Fig. S2. It was found that all nanoparticles with different contents for each size of Au nanoparticle could interact with erythrocytes. However, when comparing with the Au contents in the erythrocytes and plasma, it can be observed that the PEGylated
85 AuNPs with the 30 nm PEGylated AuNPs are more prone to interact with erythrocytes. All these results demonstrated that PEGylated AuNPs could interact with erythrocyte and may affect its membrane topography, resulting in changing the membrane structure and deformability of membrane. The turbulences in the
90 membrane integrity of erythrocytes could possibly further induce oxidative stress, which are closely associated with many diseases, such as cardiovascular diseases, stroke, and ischemic diseases etc[28]. To evaluate whether AuNPs induced turbulence of erythrocytes membrane can also induce oxidative stress, the
95 amount of malondialdehyde (MDA), a marker of lipid peroxidation, in the AuNPs treated erythrocytes was measured (Fig. 3a). As expected, erythrocytes exposed to PEGylated AuNPs, irrespective of the size, showed increased oxidation compared to that of the controls as detected by the increase in
100 malonaldehyde (MDA) levels in the cells. In addition, many previous studies have been demonstrated that the oxidative stress of cells induced by AuNPs was closely related with the overproduction of reactive oxygen species, which would damage the DNA, oxidize the polyunsaturated fatty acids and
105 amino acids in protein[29, 30], thereby inducing cell and tissue damage. In the current study, we observed that the PEGylated AuNPs could induce the lipidoxidation of erythrocytes, suggesting that the oxidative stress in PEGylated AuNPs treated erythrocytes was also derived from the overproduction
110 of reactive oxygen species. It can be speculated that the peroxidation of lipids (the product of the oxidative stress induced by AuNPs) in cell membrane induced by PEGylated AuNPs may further oxidatively damage erythrocytes membrane and disrupt fluidity and permeability as well as the deformability.

The band 3 aggregation induced by PEGylated AuNPs. On the other hand, band 3 is an important structural component of the erythrocyte cell membrane, making up to 25% of the cell membrane surface. The main functions of band 3 are modulating the binding between cytoskeleton and lipid bilayer, as well as the generation of ATP. The former is involved in ion homeostasis and cell deformability, and the latter regulates oxygen binding to hemoglobin and releasing from hemoglobin[31, 32]. As reported, reduced deformability of erythrocytes is an important feature in inflammation, also mediated by band 3, as well as nitric oxide and ROS[33]. ROS can lead to protein degradation in erythrocytes and in particular degradation of membrane protein such as band 3 and spectrin[34]. As aforementioned, the PEGylated AuNPs can induce the oxidative damage and deformability of erythrocytes, it is therefore necessary to evaluate whether the band 3 would also be affected by PEGylated AuNPs. Once the band 3 aggregated, the function of erythrocytes would be affected. As shown in Fig. 3b, when erythrocytes were pretreated with different sizes of PEGylated AuNPs at the same concentration, the expression of oligomerized band 3 were all increased remarkably compared to control group. According to previous studies, the increase in band 3 oligomerization may be induced by the dissociation of band 3 from cytoskeleton[35]. In addition, band 3 mediated decreased linkage between lipid bilayer and cytoskeleton could be enough to cause release of vesicles, which *in vivo* can act as an integral part of the physiological aging process[36]. According to the results in this study, it can be inferred
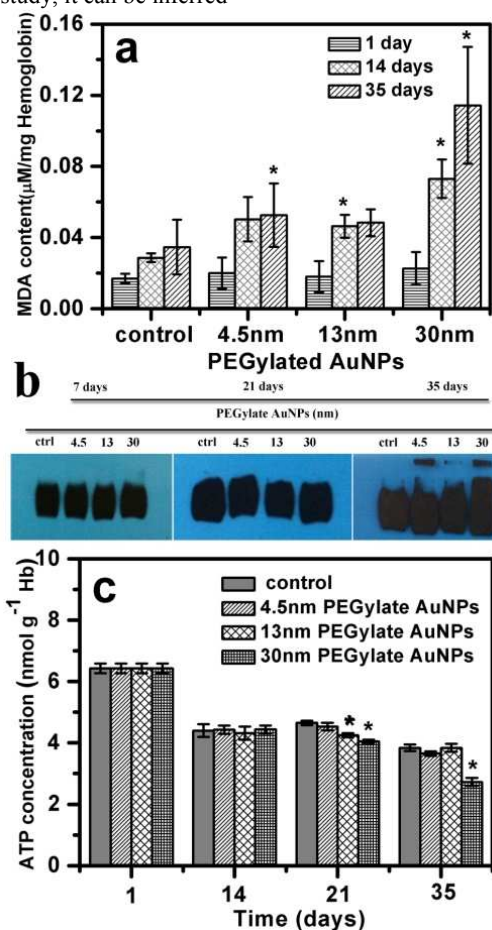
Figure 3. The impact of PEGylated AuNPs on the membrane of erythrocytes. (a) The malodialdehyde (MDA) concentrations in the erythrocytes exposed to PEGylated AuNPs. (b) Effects of PEGylated AuNPs on the aggregation levels of band 3 proteins of erythrocytes. Erythrocytes were treated with PEGylated AuNPs (200 μg ml^{-1}) for 7, 21, 35 days, respectively. Membrane were isolated and membrane proteins were separated on SDS-PAGE (10% separating gel). The band 3 protein was analyzed by Western blot; (c) The ATP concentrations in the erythrocytes exposed to PEGylated AuNPs. The data represent the means ±SEM. A statistically significant difference compared with the control is indicated by *($p<0.05$).

that PEGylated AuNPs have a greater influence on band 3 clustering, thus possibly accelerating senescent process of erythrocytes. Moreover, the concentrations of intracellular ATP (Fig. 3c) treated by PEGylated AuNPs were coincident with the band 3 assay, which showed that compared with control group, the concentration of intracellular ATP pretreated by PEGylated AuNPs decreased significantly. All these results indicated that PEGylated AuNPs, irrespective of their different sizes, may affect the deformability of erythrocyte by inducing band 3 clustering and intracellular ATP decrease. Surprisingly, compared with 4.5 and 13 nm PEGylated AuNPs, the 30 nm PEGylated AuNPs have a greater impact on the bands 3 aggregation and ATP decrease of erythrocyte. Further study on the mechanism why the 30 nm PEGylated AuNPs have a great impact on the aggregation of band-3 and the ATP decrease of erythrocytes is under process.

Effect of PEGylated AuNPs on the life span of erythrocytes. Previous studies have demonstrated that the decreased deformability of erythrocytes would shorten life span of erythrocyte in bloodstream[37]. Considering that the erythrocytes deformability was affected by PEGylated AuNPs, it is therefore necessary to evaluate whether the PEGylated AuNPs could regulate the survival of erythrocytes. Mammalian erythrocytes can produce "markers of self" (regulators) that protect them from elimination by immune system. One of these regulators, CD47, is a well-documented protein marker stably imbeds into erythrocytes membrane and is capable of inhibiting macrophage phagocytosis through interacting with the signal regulatory protein alpha (SIRPα) receptor. It is evident that CD47-deficient cells would be rapidly destroyed by SIRPα expressing leukocytes. Thus, CD47 can be used as a marker for the erythrocytes survival[38]. Based on the above description, in the current study, the CD47 expression of erythrocytes in the absence or presence of PEGylated AuNPs was investigated. The flow cytometry results showed that approximately 5% decline of CD47 expression in all PEGylated AuNPs treated groups after long time incubation (Fig. 4a). Interestingly, group comparison between negative control and AuNPs groups with different sizes reveal significant difference of CD47 expression: PEGylated AuNPs incubation leads to the loss of CD47 on erythrocytes membrane, which was much more obvious in 30nm PEGylated AuNPs group. These results demonstrated that the PEGylated AuNPs might influence the survival of erythrocytes through affecting the CD47 expression. Further considering that the deficiency of CD47 may accelerate the excessive destruction of erythrocytes by

SIRPα expressing leukocytes, it can be reasonable speculation based on the above results that PEGylated AuNPs could possibly accelerate erythrocytes clearance by increasing SIRPα expressing leukocytes in blood circulation, thereby increasing burden of immune system and leading to PEGylated AuNPs deposition in the liver and spleen[39]. In short, it is inferred that PEGylated AuNPs can accelerate senescence of erythrocytes, leading to the clearance by SIRPα expressing leukocytes in bloodstream.
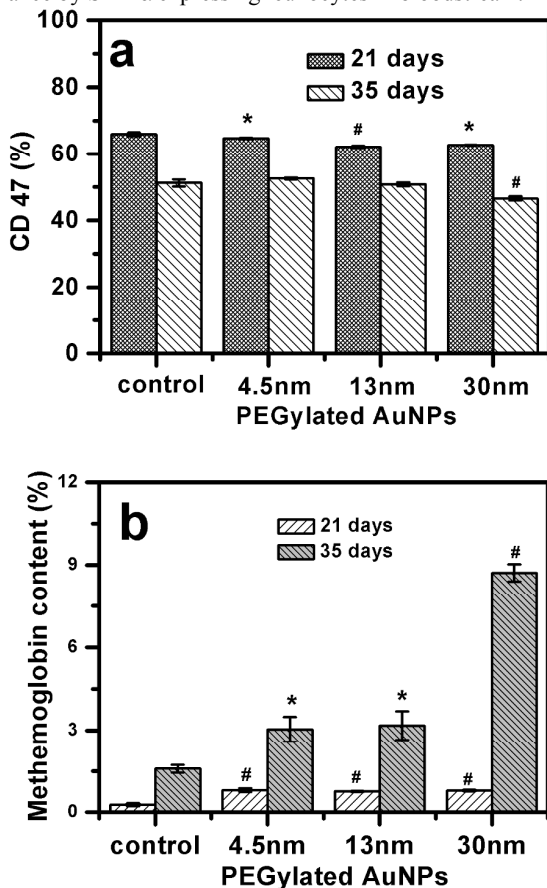
Figure 4. The effect of PEGylated AuNPs on the survival and oxygen-delivering ability of erythrocytes. (a) CD47 expression on erythrocytes pretreated by PEGylated AuNPs. Erythrocytes were treated 21 or 35 days with PEGylated AuNPs following by flow cytometry analysis; (b) The concentration of hemoglobin of erythrocytes treated by PEGylated AuNPs.

Influence of PEGylated AuNPs on erythrocytes oxygen-delivery ability. Furthermore, previous study showed that the deformability of erythrocytes generally would further impair the efficiency of oxygen delivery to the body tissue[10]. Next, we evaluate whether the oxygen-delivering ability of erythrocytes is affected when treated by PEGylated AuNPs. As shown in Table S1, there is an apparently decrease of P_{50} (~6%) in PEGylated AuNPs (4.5, 13, 30 nm) treated erythrocytes after 21 days of incubation, in contrast to control group. In terms of 13 and 30 nm PEGylated AuNPs, there is apparent decline in the oxygen-delivering ability after 14 days incubation. However, after 35 days incubation, there is no significant different between control group and PEGylated AuNPs treated group with regard to the oxygen-delivering ability. The reason, we speculated, may be that

after long time storage, the 2, 3-diphosphoglycerate presented in the erythrocytes (negative control group) were also lost, thereby leading to the decrease of oxygen-delivering ability. In addition, we measured the content of methemoglobin in erythrocytes to assay potential oxidative stress of AuNPs towards intracellular components. Our data demonstrated that the content of methemoglobin in AuNPs-treated erythrocytes (Fig. 4b, Fig. S3) was much higher than that of untreated group, which was independent of particle size. Specifically, there is apparent difference between PEGylated AuNPs treated groups and control group on the methemoglobin after 21 days (Fig. 4b). While, the content of methemoglobin in the PEGylated AuNPs-treated (especially 30 nm) erythrocytes after 35 days was significantly increased, indicating that the larger size of AuNPs would affect oxygen-carrying capacity through decrease of P_{50} and rise the content of methemoglobin in erythrocytes. As aforementioned, PEGylated AuNPs have long circulating time in the body (over one month), due to which might also lead to decrease oxygen-delivering ability of erythrocytes by PEGylated AuNPs treatment. These changes may further affect the ability of erythrocytes to deliver oxygen to the tissues, possibly resulting in the organ dysfunction and hypoxia[40].

Conclusions

Although most current studies have proved that PEGylated AuNPs are biocompatible and nontoxic both *in vitro* and *in vivo*, in this study, we uncovered the potential adverse effects of PEGylated AuNPs on the normal function of erythrocytes. The results showed that both the deformability and oxygen-delivering ability of erythrocytes are decreased treated by different sizes of PEGyalted AuNPs. Moreover, PEGylated AuNPs might shorten the life time of erythrocytes through decreasing the CD47 expression. In addition, the result also showed that the effect of PEGylated AuNPs on the primary function of erythrocytes is size-dependent. Taken together, it could be concluded that the potential impacts of PEGylated AuNPs on the function of erythrocytes should be considered before their *in vivo* application.

Experimental details

Synthesis and characterization of Au nanoparticles. Citrate-coated Au nanoparticles with 13 nm and 30 nm in diameters were synthesized as previously reported[41], PEGylated 13 nm and 30 nm Au nanoparticle were prepared by reacting citrate-coated Au nanoparticles with a 2500-fold excess of PEG-5000 for 3 h at 25 °C. The PEGylated AuNPs were synthesized according to our previous study. The morphology and size of PEGylated AuNPs were evaluated using transmission electron microscopy (TEM, JEM-200CX, Jeol Ltd., Japan). The nanoparticles surface charge (zeta potential, mV) and size distribution were determined using a ZetaSizer Nano series Nano-ZS (Malvern Instruments Ltd., Malvern, UK). The suspensions were sonicated for 5 min before use.

The hemolysis assay. Leukoreduced blood (3ml) was mixed with three different sizes of AuNPs(4.5nm, 13nm, 30nm) at various final concentrations(50, 100, 150, 200, 300 μg ml^{-1}). PBS (pH 7.4, 0.1M) was used instead of AuNPs as negative control. The

blood mixture was gently vortexed and incubated at room temperature for 2 hours.

To determine hemoglobin (Hb) levels in the plasma, blood samples were centrifuged at 3000g for 10 minutes at 4°C. Then the supernatant was further centrifuged (15000g for 30min) in order to remove PEGylated AuNPs from plasma. And supernatant Hb levels were measured by three wavelengths method ： supernatant Hb （ mg/L ） =[1.68×A$_{415}$- 0.84×(A$_{380}$+A$_{450}$)] ×1000 mg ml^{-1} [36,37]. Total Hemoglobin (HGB) and hematocrit (HCT) were analyzed by auto hematology analyzer (BC-5800, Mindray Corp., Shenzhen, China). Hemolytic rate (%) was calculated using a standard formula:

Hemolytic rate (%) = (supernatant Hb×[1-Hct%])/total Hb×100.

Hemolytic rate of whole blood must be lower than 1% by FDA regulations (European <0.8%, China <0.8%). Based on hemolysis assay results, PEGylated AuNPs concentration for further experiments was designated as 200μg ml^{-1}.

Detection of intracellular ATP levels in erythrocytes. Erythrocytes intracellular ATP levels were measured using a firefly luciferase-based ATP assay kit (Beyotime, China) according to manufacturer's instructions. Briefly, after erythrocytes washed and lysised on ice, the diluent was mixed with ATP detection working dilution. Luminance (RLU) was measured by a luminometer (Centro LB 960, Berthold technologies Corp.,), and hemoglobin concentration of samples were measured by orthotolidine method. Finally, ATP levels were expressed as μmol mg^{-1} Hb.

Erythrocytes deformability assay. Erythrocytes deformability was analyzed by a Laser-diffraction Ektacytometer (LBY-BX, Beijing Precil Instrument Co., Ltd, China) according to the manufacturer's manual. In brief, approximately 20μl blood was suspended in 1ml PBS containing 15% polyvinylpyrrolidone. A thin layer of the RBC suspension was sheared between two concentric cylinders (size of the gap was 0.5 mm) at four different shear stresses (0.39, 0.77, 1.54, and 7.7 Pa) at 37°C. The shear rate was increased by a faster rotation of the outer cup to cause RBC deformation, and erythrocytes deformability was detected at four different Shearing forces according to laser diffraction principle.

Morphological studies of red blood cells. RBCs were pipetted from bloods that incubated with different diameter AuNPs at different time points. After washed with PBS, RBCs were diluted to 5% hematocrit with PBS(including 2% glutaraldehyde, 3ml) and mica plates were added to incubation for 2 hours. RBCs were fixed to mica plates by natural sedimentation due to gravity. Mica plates were then dehydrated in increasing concentrations of ethanol (25, 50, 75, 90, and 100%) for 15 min each. The plates were dried, and coated with Au before viewing under a scanning electron microscope (model quanta250; FEI Ltd., USA).

Purification of Human RBC Ghosts proteins. RBCs were washed with phosphate-buffered saline (PBS) for three times, and 1 ml Packed RBCs were lysed for 1 hour in 50ml of hypotonic lysing solution containing 0.01M Tris, 0.02mM PMSF, and cocktail inhibitor, pH 7.4, at 4°C to reduce premature, spontaneous resealing of the erythrocyte ghosts. The membranes were then centrifuged at 10,000 × g for 30 min at 4°C. After discarding the supernatant, the membranes were then washed in 50 ml of hypotonic lysing solution and recentrifuged at 10,000 ×

g for 30 min at 4°C. And repeat this step for three times. After removing the supernatant of the final time, the erythrocyte ghost membranes were suspended in lysing solution. The concentration of RBC ghosts protein was determined by Bradford protein assay kit (Beyotime, China). And all samples were adjusted to 0.5mg/ml with distilled water.

SDS-PAGE and Western Blot Analysis of band3 protein. Aliquots of RBC ghost proteins were separated by 10% SDS-PAGE, each lane contains 4μg protein. Then the proteins were transferred to PVDF membrane. After blocked for 10h in blocking buffer (10mM Tris, pH7.4, 150mM NaCl, 0.5%Tween 20, 3% Bovine Serum Albumin), the blot was probed for 4h with the band3 primary antibodies(mouse anti-human, Sigma-Aldrich). After several washes, the blot was incubated with bovine anti-mouse IgG coupled to HRP(Santa Cruz) for 2h. After several washes, the PVDF membrane was detected with the Super Signal West Pico chemiluminescence detection kit(Thermo scientific).

Statistical analysis. Results are expressed as means ± SEM. Statistical significance among groups was determined by *t*-test, ANOVA (analysis of variance). Probability values of p<0.05 were considered significant.

Acknowledgement

Notes and references

[a] *Institute of Blood Transfusion, Chinese Academy of Medical Sciences and Peking Union Medical College, 610052 Chengdu, P. R. China. E-mail: jxliu8122@vip.sina.com*
[b] *State Key Laboratory for Structural Chemistry of Unstable and Stable Species, Center for Molecular Sciences, Institute of Chemistry, Chinese Academy of Sciences. 100190 Beijing, P. R. China. Fax: +861062559373; Tel: +861062566306; E-mail: dulibo@iccas.ac.cn*
† Electronic Supplementary Information (ESI) available: [details of any supplementary information available should be included here]. See DOI: 10.1039/b000000x/

Reference

1 Boisselier, E.; Astruc, D. Gold nanoparticles in nanomedicine: preparations, imaging, diagnostics, therapies and toxicity. *Chem. Soc. Rev.* **2009**, *38*, 1759-1782.

2 Chen, Y.; Samia, A. C.; Meyers, J. D.; Panagopoulos, I.; Fei, B.; Burda, C. Highly efficient drug delivery with gold nanoparticle vectors for *in vivo* photodynamic therapy of cancer. *J. Am. Chem. Soc.* **2008**, *130*, 10643-10647.

3 Dreaden, E. C.; Alkilany, A. M.; Huang, X.; Murphy, C. J.; Mostafa A. EI-S. The golden age: gold nanoparticles for biomedicine. *Chem. Soc. Rev.* **2012**, *41*, 2740-2779.

4 Goel, R.; Shah, N.; Visaria, R.; Paciotti, G. F.; Bischof, J. C. Biodistribution of TNF-α-coated gold nanoparticles in an *in vivo* model system. *Nanomedicine (Lond).* **2009**, *4*, 401-410.

5 Davis, M. E.; Zuckerman, J. E.; Choi, C. H. J.; Seligson, D.;

Tolcher, A.; Alabi, C. A.; Yen, Y.; Heidel, J. D.; Ribas, A. Evidence of RNAi in humans from systemically administered siRNA via targeted nanoparticles. *Nature* **2010**, *464*, 1067-1070.

6   Liu, Z.; Li, W.; Wang, F.; Sun, C.; Wang, L.; Wang, J.; Sun, F. Enhancement of lipopolysaccharide-induced nitric oxide and interleukin-6 production by PEGylated gold nanoparticles in RAW264.7 cells. *Nanoscale*, **2012**, *4*, 7135-7142.

7   Cho, W-S.; Cho, M.; Jeong, J.; Choi, M.; Han, B. S.; Shin H-S.; Hong, J.; Chung, BH.; Jeong, J.; Cho, M-H. Size-dependent tissue kinetics of PEG-coated gold nanoparticles. *Toxicol. Appl. Pharmacol.* **2010**, *245*, 116-123.

8   Khlebtsov, N.; Dykman, L. Biodistribution and toxicity of engineered gold nanoparticles: a review of *in vitro* and *in vivo* studies. *Chem. Soc. Rev.* **2011**, *40*, 1647-1671.

9   Yang, H.; Sun, C.; Fan, Z.; Tian, X.; Yan, L.; Du, L. et al. Effects of gestational age and surface modification on materno-fetal transfer of nanoparticles in murine pregnancy. *Sci. Rep.* **2012**, *2*, 847.

10   Krantz, S. B. Erythropoietin. *Blood* **1991**, *77*, 419-434.

11   Orhan, H.; Evelo, C.T.A.; Sahin, G. Erythrocyte antioxidant defense response against cigarette smoking in humans-the glutathione S-transferase vulnerability. *J. Biochem. Mol. Toxic.* **2005**, *19(4)*, 226-233.

12   Turkez, H.; yousef, M.I.; Sönmez, E.; Togar, B.; Bakan, F.; Sozio, P.; Stefano, A.D. Evaluation of cytotoxic, oxidative stress and genotoxic responses of hydroxyapatite nanoparticles on human blood cells. *J. Appl. Toxicol.* **2014**, *34*, 373-379.

13   Shi, J.; Hedberg, Y.; Lundin, M.; Odnevall Wallinder O.; Karlsson, H. L.; Möller, L. Hemolytic properties of synthetic nano- and porous silica particles: The effect of surface properties and the protection by the plasma corona. *Acta Biomaterialia,* **2012**, *8*, 3478-3490.

14   Li, S. Q.; Zhu, R. R.; Zhu, H.; Sun, X. Y.; Yao, S. D.; Wang, S. L. Nanotoxicity of TiO2 nanoparticles to erythrocyte *in vitro*. *Food Chem. Toxicol.* **2008**, *46*, 3626-3631.

15   Slowing, I. I.; Wu, C. W.; Vivero-Escoto, J. L.; Lin, V. S. Mesoporous silica nanoparticles for reducing hemolytic activity towards mammalian red blood cells. *Small* **2009**, *5*, 57-62.

16   Shah, N. B.; Vercellotti, G. M.; White, J. G.; Fegan, A.; Wagner, C. R.; Bischof, J. C. Blood-nanoparticle interactions and *in vivo* biodistribution: impact of surface PEG and ligand properties. *Mol. Pharmaceutics.* **2012**, *9*, 2146-2155.

17   Sultana, S.; Khan, M. R.; Kumar, M.; Kumar, S.; Ali, M. Nanoparticles-mediated drug delivery approaches for cancer targeting: a review. *J. Drug. Target.* **2013**, *21*, 107-125.

18   Garratty G. Immune hemolytic anemia associated with drug therapy. *Blood Rev.,* **2010**, *24*, 143-150.

19   Schaer, D. J.; Buehler, P. W.; Alayash, A. I.; Belcher, J. D.; Vercellotti, G. M. Hemolysis and free hemoglobin revisited: exploring hemoglobin and hemin scavengers as a novel class of therapeutic proteins. *Blood*, **2013**, *121*, 1276-1284.

20   Nimi, N.; Paul, W.; Sharma, C. P. Blood protein adsorption and compatibility studies of gold nanoparticles. *Gold Bull.* **2011**, *44*, 15-20.

21   Prencipe, G.; Tabakman, S. M.; Welsher, K.; Liu, Z.; Goodwin, A. P.; Zhang, L.; Henry, J.; Dai, H. PEG branched polymer for functionalization of nanomaterials with ultralong blood circulation. *J. Am. Chem. Soc.* **2009**, *131*, 4783-4787.

22   Parthasarathi, K.; Lipowsky, H. H. Capillary recruitment in response to tissue hypoxia and its dependence on red blood cell deformability. *Am. J. Physiol.* **1999**, *277*, H2145-H2157.

23   Marossy, A.; Svorc, P.; Kron, I.; Gresova, S. Hemorheology and circulation. *Clin. Hemorheol. Microcirc.* **2009**, *42*, 239-258.

24   McHedlishvili, G. Disturbed blood flow structuring as critical factor of hemorheological disorders in microcirculation. *Clin. Hemorheol. Microcirc.* **1998**, *19*, 315-325.

25   Yawata, Y. Cell Membrane: the Red Blood Cell as a Model. pp 38-40 (Wiley-VCH: Weinheim, Germany, 2003).

26   Delaunay, J. The molecular basis of hereditary red cell membrane disorders, *Blood Rev.* **2007**, *53*, 61-70.

27   Pretorius, E., Kell, D. B. Diagnostic morphology: biophysical indicators for iron-driven inflammatory diseases. *Integr. Biol.* **2014**, *6*, 486-510.

28   Wilson, W. R.; Hay, M. P. Targeting hypoxia in cancer therapy. *Nat Rev. Cancer,* **2011**, *11*, 393-410.

29   Li, J.J.; Hartono, D.; Ong, C.-N.; Bay, B-H.; Yung, L-Y. Autophagy and oxidative stress associated with gold nanoparticles. *Biomaterials*, **2010**, *31*, 5996-6003.

30   Pan, Y.; Leifert, A.; Ruau, D.; Neuss, S.; Bornemann, J.; Schmid, G.; Brandau, W.; Simon, U.; Jahnen-Dechent, W. Gold nanoparticles of diameter 1.4 nm trigger necrosis by oxidative stress and mitochondrial damage. *Small*, **2009**, *5*, 2067-2076.

31   Lewis, I. A., Campanella, M. E.; Markley, J. L.; Low, P. S. Role of band 3 in regulating metabolic flux of red blood cells. *Proc. Natl. Acad. Sci. USA* **2009**, *106*, 18515-18520.

32   Bosman, G. J. C. G. M.; Stappers, M. ; Novotnỳ. V. M. J. Changes in band 3 structure as determinants of erythrocyte integrity during storage and survival after transfusion. *Blood Transfus.* **2010**, *8* (Suppl 3), S48-S52.

33   Straat, M.; Van Bruggen, R.; De Korte, D.; Juffermans, N.P. Red blood cell clearance in inflammation. *Transfus. Med. Hemother.* **2012**, *39*, 353-361.

34   Uyesaka, N.; Hasegawa, S.; Ishioka, N.; Ishioka, R.; Shio, H.; Schechter, A.N. Effects of superoxide anions on red cell deformability and membrane proteins. *Biorheology*, **1992**, *29*, 217-229.

35   Karon, B. S.; Hoyer, J. D.; Stubbs, J. R.; Thomas, D. D. Changes in band 3 oligomeric state precede cell membrane phospholipid loss during blood bank storage of red blood cells. *Transfusion* **2009**, *49*, 1435-1442.

36   Willekens, F. L. A.; Were, J. M.; Groenen-Dopp Y. A.; Roerdinkholder-Stoelwinder B.; DePauw, B.; Bosman, G. J. Erythrocyte vesiculation: a self-protective mechanism? *Brit.*

Nanoscale Accepted Manuscript

J. Haematol. **2008***, 141*, 549-556.

37 Khandelwal, S.; Rooijen, N. V.; Saxena, R. K. Reduced expression of CD47 during murine red blood cell (RBC) senescence and its role in RBC clearance from the
5   circulation. *Transfusion*, **2007**, *47*, 1725-1731.

38 Oldenborg, P-A.; Zhelenznyak, A.; Fang, Y. F.; Lagenaur, C. F.; Gresham, H. D.; Lindberg, F. P. Role of CD47 as a marker of self on red blood cells. *Science* **2000**, *288*, 2051-2054.

10 39 Lipka, J.; Semmeler-Behnke, M.; Sperling, R. A.; Wenk, A.; Takenaka, S.; Schleh, C.; Kissel, T.; Parak, W. J.; Kreyling, W. G. Biodistribution of PEG-modified gold nanoparticles following intratracheal instillation and intravenous injection. *Biomaterials* **2010**, *31*, 6574-6581.

15 40 Hakim, T. S.; Macek, A. S. Role of erythrocyte deformability in the acute hypoxic pressor response in the pulmonary vasculature. *Respir. Physiol*. **1988**, *72*, 95-107.

41 Yang, H.; Sun, C.; Fan, Z.; Tian, X.; Yan, L.; Du, L.; Liu, Y.; Chen, C.; Liang, X.-J.; Anderson, G. J.; Keelan, J.A.; Zhao,
20   Y.; Nie, G. Effects of gestational age and surface modification on materno-fetal transfer of nanoparticles in murine pregnancy, *Scientific Report*, **2012**, *2*, 847